
The Influence of Flood Source Placement on Radiation Exposure During Quality Control Testing

Mark J. Rudin and William H. Johnson

Department of Health Physics, University of Nevada–Las Vegas, Las Vegas, Nevada

Objective: This study examined the photon energy distribution and exposure rate from a 250-MBq ^{57}Co flood source during quality control (QC) procedures as a function of source placement and measurement location. The optimum placement of the source to reduce the radiation dose to the nuclear medicine technologist during QC checks was determined.

Methods: Measurements of exposure rate were made inside and outside a camera room with the source positioned either above or below the camera head. The energy distribution of the photon field was examined at the same locations using a high-resolution gamma-ray spectrometer. Additional measures of exposure rate were made with the source at various distances from the camera face.

Results: The lowest exposure rates occurred when the source was lying directly on the face of the camera head. The exposure rates at locations inside the camera room increased by a factor of 4.3 ± 3.0 when the source was placed on an imaging table below the camera head. This increase can be attributed to decreased shielding provided by the camera head.

Conclusion: A large portion of the radiation dose received by technologists during QC checks is due to scattered radiation and x-rays produced by gamma-ray interactions within the camera. This dose can be reduced significantly if QC checks are performed with the flood source lying directly on the inverted gamma camera head rather than placing the flood source on an imaging table under the gamma camera.

Key Words: technologist radiation dose; cobalt-57 flood source; quality control procedures

J Nucl Med Technol 2000; 28:88–93

Flood sources containing 185–370 MBq ^{57}Co are used routinely in nuclear medicine facilities to check the uniformity response and spatial resolution of scintillation cameras. Extrinsic uniformity checks involve placing the ^{57}Co flood source on an inverted detector head with the collimator in place and accumulating 2–3 million counts, depending on the type of instrumen-

tation being used (1). Intrinsic uniformity checks are performed without a collimator and are an alternative to extrinsic checks, although only the detector and the associated electronics are evaluated. Intrinsic checks are performed with a low-activity point source placed 5 useful fields of view away from the camera face (2,3). It is recommended that uniformity checks be performed daily (1,2). Extrinsic spatial resolution and linearity checks with bar phantoms are performed typically on a weekly basis (1,2). On days when all of these quality control (QC) tests are conducted, a flood source may be unshielded for up to 30 min at a time.

Several authors have attempted to quantify the dose received by nuclear medicine technologists from procedures, including radiopharmaceutical preparation and handling, and QC checks using flood phantoms and point sources (4–9). There is little or no information on the characteristics of the radiation dose that nuclear medicine personnel might receive in terms of its energy distribution. The purposes of this study were to compare exposure rate measurements and the corresponding gamma-ray spectra obtained during the use of a solid ^{57}Co disk source and to identify methods of reducing technologist radiation doses during QC procedures.

MATERIALS AND METHODS

This study was conducted in a nuclear medicine teaching laboratory. The facility is located on the ground level of a 5-story building and houses a large field-of-view single-head gamma camera system (Model 300SX, Picker International, Inc., Cleveland, OH) that is oriented in the room as shown in Figure 1. Access to the rooms directly to the east of the main imaging area is restricted to nuclear medicine personnel only. The areas outside the west and south walls are public hallways, while a parking area is located just outside the north wall of the facility. The room directly above the facility is a classroom that is occupied approximately 20% of the time.

The nuclear medicine laboratory was designed originally to be an ultrasound imaging teaching laboratory. No special efforts were taken during design to shield the laboratory. The exterior of the north wall facing the parking lot and a portion of the west wall (north of the outer entrance door) is constructed with 20-cm thick concrete blocks. The interior of these walls is a

For correspondence or reprints contact: Dr. Mark J. Rudin, Department of Health Physics, University of Nevada, Las Vegas, 4505 Maryland Pkwy., Las Vegas, NV 89154–3037; Phone: 702–895–3299; E-mail: mrudin@cmail.nevada.edu.

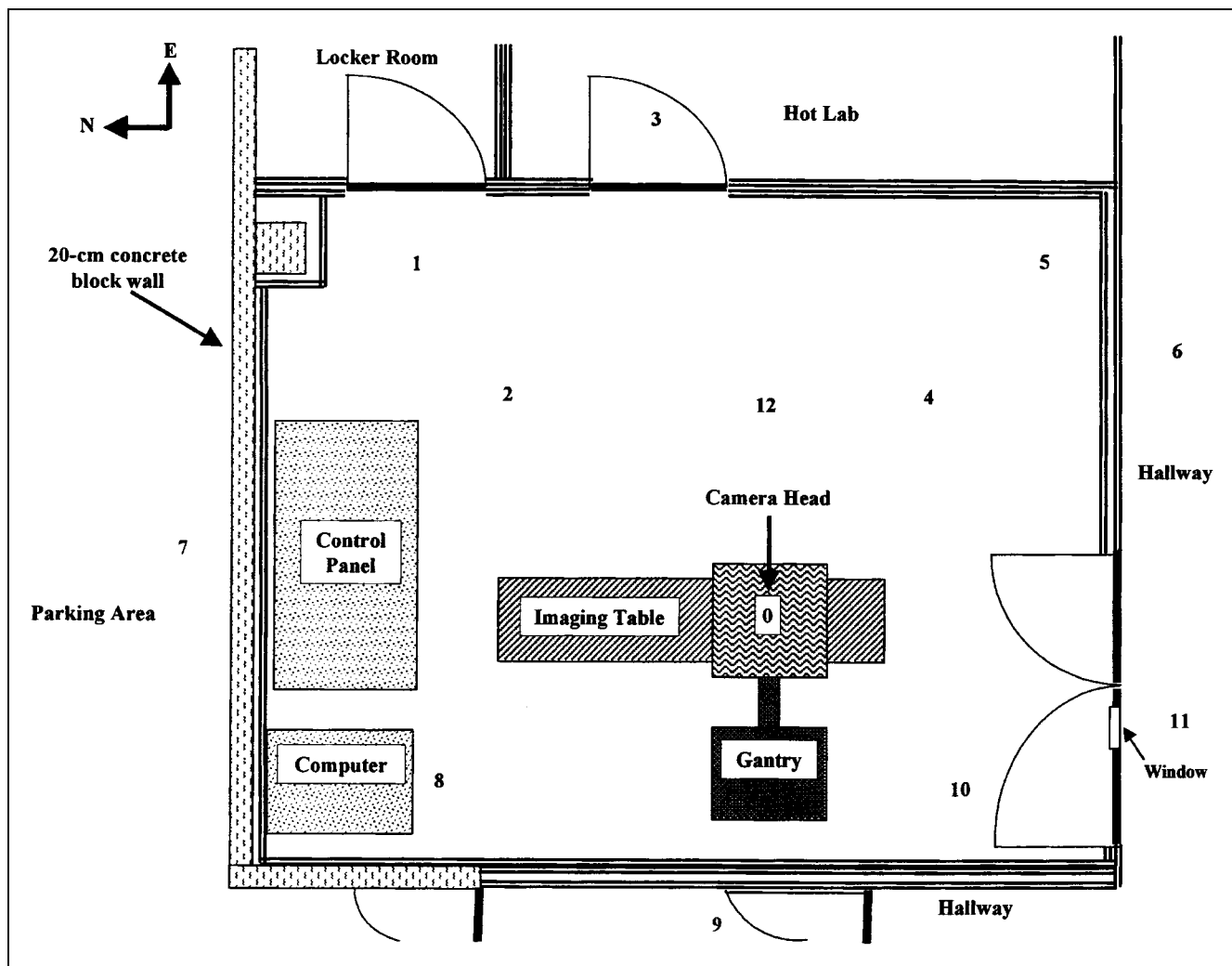


FIGURE 1. Schematic view of a nuclear medicine laboratory showing measurement locations.

1.6-cm-thick sheet of type-X gypsum board mounted on 5-cm metal studs. The other walls consist of a 1.6-cm-thick sheet of type-X gypsum board mounted on each side of 9.2-cm metal studs. Between the gypsum board sheets is 8.8 cm of mineral fiber instillation. The section of the west wall, south of the concrete block wall, has an additional layer of 1.6 cm of gypsum board on the laboratory side. All doors leading into the room are hollow, wooden doors, 4 cm thick. The door between the camera room and the hallway has a glass window.

Two exposure scenarios typically encountered during QC testing in nuclear medicine facilities were simulated in this study. Each used a circular 250-MBq ^{57}Co flood source made with an epoxy matrix on a thermoplastic backing. It had a total area of 0.34 m² and an active area of 0.29 m². At the time of the study, the flood source contained trace amounts of ^{56}Co and ^{58}Co ; each being less than 0.05% of the total activity. The face of the camera head was rectangular with an area of 0.22 m² and had a collimator attached. In the first scenario, the source was placed on the inverted (face up) camera head. The distance from the top of the camera head to the floor measured 1.5 m. The second exposure scenario involved placing the same flood source on an imaging table (overlaid with a 2.5-cm foam pad)

and centering the source directly under the camera head (face down). The distance from the bottom of the camera face to the floor was 1.0 m. Care was taken to ensure the camera face and flood source were less than 2 cm apart.

During each exposure scenario, photon energy spectra were collected from selected areas inside and outside the imaging room using an energy-calibrated high-purity germanium (HPGe) gamma-ray spectroscopy system. The approximate sampling locations (Locations 1 through 11) are presented by number in Figure 1. The spectroscopy system used an unshielded detector with 40% relative efficiency with a 4096-channel multichannel analyzer calibrated to approximately 0.5 keV per channel (Oxford Instruments [now Canberra Industries, Inc.], Meriden, CT). The electronics of the spectroscopy system were kept in an adjacent room to minimize radiation scattering off the electronics package. Thirty-minute count times were used to ensure a sufficient number of counts were collected so the 122- and 136-keV photoelectric peaks for ^{57}Co could be differentiated.

The center of the sensitive volume of the HPGe detector was at a height of 0.9 m from the floor. Because of the relatively large distances from the source to where the measurements were taken, there is little difference in the source-to-detector

distance between the 2 scenarios. Raising the source 0.5 m in the camera face-up scenario, resulted in a less than 4% increase in source-to-detector distance at all locations except Location 4. At Location 4, the difference in distance was 16%.

The performance of a gamma-ray spectrometry detector often is described by its peak-to-Compton ratio (PTCR). This ratio typically is used to represent the ability of a germanium detector to properly sense the energy of an incoming gamma ray. It is a measure of the combined effects of detector energy resolution and the photofraction (10). The PTCR is defined for a ^{60}Co source and is determined by dividing the total counts in the peak channel of the 1332-keV peak by the average counts per channel in the flat portion of Compton continuum (1040–1096 keV) associated with that peak (11,12). Based on this definition, the detector used in this study had a PTCR of 72.2. The PTCR of a detector varies with detector size. For a given detector and source configuration, the PTCR decreases if there are nearby structures that may scatter gamma rays into the detector.

In this study, PTCR was operationally defined for a ^{57}Co flood source. Using the 122-keV peak of ^{57}Co , the PTCR was defined as the counts in the highest channel of the peak divided by average counts per channel in the Compton continuum (17–41 keV). Figure 2 depicts the portions of the spectrum used in this calculation.

A second parameter used in this study to examine the photon energy spectra was a peak-to-x-ray ratio (PTXR). The PTXR was defined as the ratio of the ^{57}Co 122-keV gamma rays to lead K_{β} x-rays detected at a given location. It was calculated by dividing the total counts in the highest channel of the 122-keV

photopeak by the counts in the highest channel of the lead $K_{\beta 1}$ x-ray peak at 85 keV.

A calibrated, Geiger-Mueller handheld survey meter (Model 14-C, Ludlum Measurements, Inc., Sweetwater, TX) with a thin-wall cylindrical detector (Model 44-6) was used to determine exposure rates at each of the sampling locations. The detector was held at a height of 0.9 m for each measurement. When taking measurements at Locations 3 and 11, the doors to the camera room were closed. The detector was calibrated using a NIST-traceable ^{137}Cs source. The detector is energy-dependent and its response to photons in the 70- to 150-keV range is too high by a factor of approximately 2.2, while it is too low for energies less than 55 keV. Because of the complex photon energy spectra being examined and the varying energy response of the detector, no attempts were made to correct the exposure rate reported by the meter.

For purposes of data comparisons, measurement locations were divided into 2 groups. The first group included locations inside the camera room (Locations 1, 2, 4, 5, 8 and 10), while the second group included locations outside the room that were shielded by walls and doors (Locations 3, 6, 7, 9 and 11). ANOVA was used to examine differences in exposure rate and photon energy spectra parameters between the 2 source placement scenarios.

The influence of the distance from the source to the camera face on exposure rate also was examined. Exposure rate measurements at a height of 0.9 m were taken at Locations 4 and 12 as the camera head was raised to varying heights above the source (camera facedown scenario).

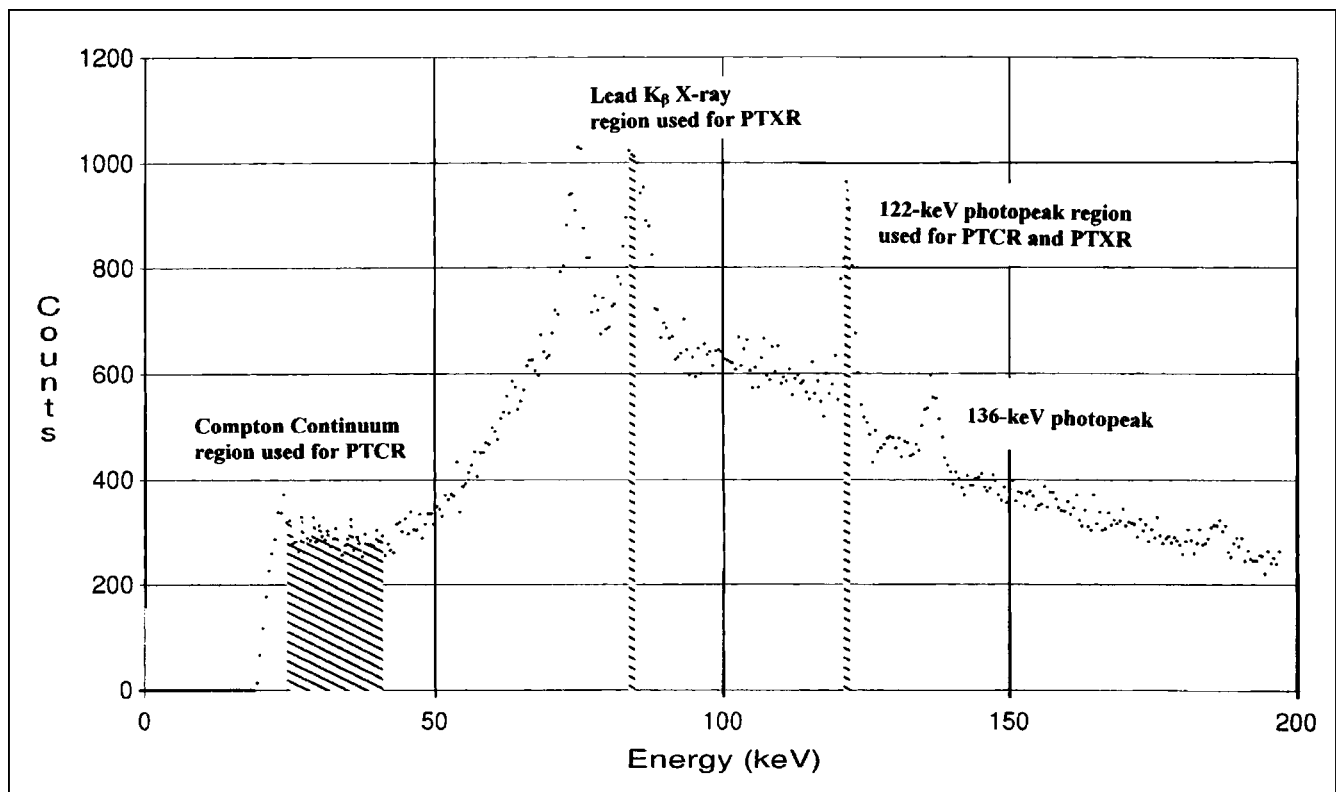


FIGURE 2. Portion of the energy spectra compared to determine the PTCR and PTXR. This is the background gamma-ray energy spectrum collected during a 30-min count at Location 9, when the source was stored in a lead-lined container in the hot laboratory.

RESULTS

Thirty-minute background spectra were collected at Locations 7 and 9 with the source stored in a lead-lined container in the hot lab. Background exposure rates taken at these locations averaged $2 \text{ pC kg}^{-1} \text{ s}^{-1}$ ($30 \text{ }\mu\text{R hr}^{-1}$). At Location 9, the resulting 122-keV peak in the background spectrum was nearly 2 orders of magnitude less than during either QC scenario. Because of the small peak height compared to natural background radiation, the PTCR at Location 9 was 8.3 ± 2.6 and the PTXR was 0.95 ± 0.04 . Although no 122-keV peak was observed in the background spectrum at Location 7, the operational definitions of PTCR and PTXR yielded values of 4.7 ± 2.6 and 0.72 ± 0.04 , respectively.

Table 1 lists the exposure rate, PTCR and PTXR at each location examined using gamma-ray spectroscopy. For locations inside the camera room, there was a significant difference in exposure rate ($P = 0.0034$), the PTCR ($P = 0.026$) and the PTXR ($P = 0.0005$) between the 2 source placement scenarios investigated. The exposure rate from the flood source increased by a factor of 4.3 ± 3.0 when the source was placed below the camera head (face down) as compared with placement of the source above the camera head (face up). The increase in exposure rates over background averaged $2.8 \pm 1.4 \text{ pC kg}^{-1} \text{ s}^{-1}$ ($39 \pm 20 \text{ }\mu\text{R hr}^{-1}$) when the flood source was lying on the camera head (face up) and $11.9 \pm 5.7 \text{ pC kg}^{-1} \text{ s}^{-1}$ ($170 \pm 79 \text{ }\mu\text{R hr}^{-1}$) when the flood source was below the camera head (face down). The average PTCR for locations in the camera room was 66.0 ± 11.0 when the flood source was above the camera (face up) and 50.2 ± 10.0 when the flood source was below the camera (face down). The smaller errors in the calculated PTCR for each location when the flood source was below the camera (face down) are due to the significantly higher count rates obtained with that geometry. The PTXR of the locations in the room averaged 2.4 ± 0.8 with the flood source above the camera (face up) compared to 5.0 ± 1.0 with the flood source below the camera (face down).

Results were varied for the locations shielded by doors and walls. The exposure was at or near background at all locations

when the flood source was above the camera (face up). The exposure rate was slightly higher at most locations when the flood source was below the camera (face down). Location 11 was an exception. The exposure rate showed a large increase when the flood source was placed below the camera (face down). This suggested that the window in the door provided relatively little shielding. The PTCR decreased at Locations 3, 6 and 11 when the flood source was placed under the detector, but increased at Location 9. At Location 7, which was shielded by the brick wall, counts obtained in the 122-keV peak were 3 orders of magnitude less than all other locations for both source positions. The PTCR of the 2-source placement scenarios at Location 7 were similar to the value observed there when the source was placed in storage (i.e., background).

The distance between the camera head and the source influenced the resulting exposure rates. When the source was below the camera (camera facedown scenario) and the distance between the source and the camera face was less than 5 cm, the camera head shielded the source resulting in a reduced exposure rate. Positioning the flood source directly on the camera face (face up) provided the greatest reduction in exposure rate. This was because the camera head more effectively shielded the source in relation to the 0.9-m high monitoring locations.

DISCUSSION

Figure 3 presents an example of the photon energy spectra observed. Differences in the size and shape of the spectra and the photon fluence rate from the two-source placement scenarios were observed readily. The peak in each spectrum at 85 keV corresponds to the K_{β} x-rays of lead. Lead x-rays are produced after gamma rays from the flood source interact through the photoelectric effect with the collimator and the shielding surrounding the camera head. The x-rays are radiated isotropically from the camera head. When the source was lying below the camera head (face down), the K_{α} x-rays of lead also were observed at 73 and 75 keV in the spectra. Because of their

TABLE 1
Exposure Rate, PTCR and PTXR Measured at Various Locations In and Around the Nuclear Medicine Laboratory

Location	Distance from source (m)	Exposure rate ($\text{pC kg}^{-1} \text{ s}^{-1}$)		Peak-to-Compton ratio		Peak-to-x-ray ratio	
		Camera facing up	Camera facing down	Camera facing up	Camera facing down	Camera facing up	Camera facing down
1	2.96	4	9	78 ± 0.5	52 ± 0.2	3.4 ± 0.02	4.9 ± 0.02
2	2.45	5	14	72 ± 0.4	62 ± 0.1	2.1 ± 0.01	5.9 ± 0.02
3	2.50	2	3	77 ± 0.5	22 ± 0.1	3.9 ± 0.03	2.9 ± 0.02
4	0.86	7	25	69 ± 0.3	59 ± 0.1	1.8 ± 0.01	6.0 ± 0.01
5	1.79	5	11	71 ± 0.4	47 ± 0.1	3.4 ± 0.02	5.0 ± 0.02
6	2.64	2	3	68 ± 0.5	36 ± 0.1	3.5 ± 0.02	3.6 ± 0.02
7	4.12	2	2	4.7 ± 0.1	5.3 ± 0.1	0.56 ± 0.02	0.70 ± 0.02
8	2.92	4	13	48 ± 0.3	34 ± 0.1	1.5 ± 0.01	3.5 ± 0.02
9	2.90	2	3	12 ± 0.1	30 ± 0.1	0.49 ± 0.01	2.6 ± 0.02
10	2.11	6	13	58 ± 0.3	47 ± 0.1	2.1 ± 0.01	4.4 ± 0.01
11	2.65	3	13	69 ± 0.4	49 ± 0.2	3.4 ± 0.02	5.2 ± 0.02

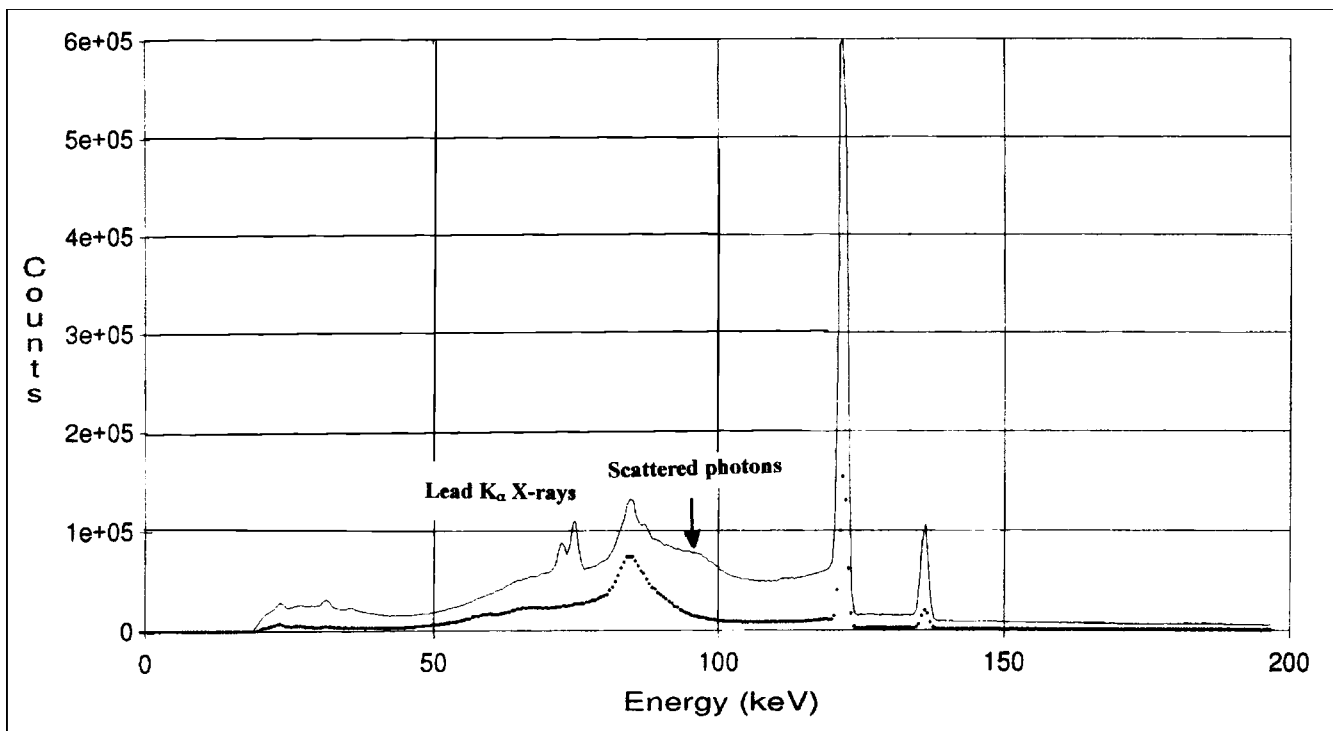


FIGURE 3. Gamma-ray spectra collected during a 30-min count at Location 2 with the flood source above (dotted line) and below (solid line) the camera.

lower energy, the probability of the K_{α} x-rays interacting before leaving the lead shielding was nearly twice that of the K_{β} x-rays. This resulted in a reduced intensity of the K_{α} x-rays compared to the K_{β} x-rays at all measurement locations. The small air gap between the source and the detector, when the source was placed below the camera (face down), was sufficient to present an unshielded path for photons to emerge from the camera head and the flood source. When the source is placed directly on the face of the camera (face up) there was no air gap. This was one of the reasons the exposure rate decreased when the source was placed above the camera.

The sharp peaks in the photon energy spectra at 122 and 136 keV were due to gamma rays emerging from the flood source and interacting directly with the detector by the photoelectric effect. These peaks were more pronounced when the flood source was below the camera head and in the same plane as the measuring devices. Placing the source above the camera head increased the fraction of gamma rays that needed to travel through the camera head to reach a measuring device. Evidence for the camera head serving as a shield when the source was placed above the camera (face up) was given by the PTXR values. The camera head reduced the gamma-ray intensity from the source, but was less effective in stopping the lead x-rays and scattered photons produced in the camera head itself. This resulted in a lower PTXR when the flood source was above the camera. It should be noted that the amount of shielding provided by the camera head would vary depending on the height of the camera face (and the source) relative to the height of the exposure rate measurement.

Compton scattering was not a major interaction mechanism in the lead shielding surrounding the camera head because the

energy of the ^{57}Co gamma rays is relatively low. Compton scattering is an interaction mechanism in lower atomic number materials, such as the camera supports. The maximum energy of the recoil electron produced during the Compton scattering of a 122-keV gamma ray is 39 keV (47 keV for a 136-keV gamma ray). The scattered photon will have an energy greater than 83 keV (89 keV for a 136-keV gamma ray).

The flat portion of the spectra at lower energies was caused by gamma rays from the source interacting with the detector through Compton scattering. Because of the low-energy of the recoil electron produced and the small probability of the reaction, Compton scattering contributes little to measured exposure rate directly. It does contribute indirectly, however. Photons scattered by structural components made of relatively low atomic number materials result in the increased counts with decreasing energy in the range 83–122 keV. These scattered photons then may interact through the photoelectric effect resulting in increased counts at lower energies.

The extra shielding provided by the walls of the camera room resulted in the PTXR for locations outside the room to be lower, on average, than at locations inside the room. This was especially evident at Location 7, which was shielded by the brick wall, and Location 9. Between Location 9 and the flood source, there was an extra layer of gypsum board and the camera gantry. At Location 9, the PTXR was lower when the flood source was above the camera (face up). The presence of lead counter weighting in the lower portion of the gantry appears to have increased the amount of shielding when the flood source was below the camera head (face down).

The change in exposure rate obtained when repositioning the flood source was not entirely due to changes in the 122-keV

gamma counting rate. A regression analysis of the ratio of counts in the 122-keV peaks in the two-source positions to the ratio of exposure rates yields an $R^2 = 0.57$. This implies that changes in the 122-keV gamma counting rate are not solely responsible for changes in exposure rate. Changes in the amount of scattered radiation and lead x-rays also contributed to the measured exposure rate and must be considered.

CONCLUSION

Attempting to calculate technologist's radiation dose from a flood source during routine QC procedures based solely on the ^{57}Co gamma rays may lead to a significant underestimation of the exposure dose. Analysis of the photon energy spectrum shows that a large portion of the dose received is from scattered photons and lead x-rays. The radiation safety principle of ALARA (as low as is reasonably achievable) dictates placing the flood source above an inverted camera head (face up) whenever possible during these procedures. This will reduce significantly the technologist's radiation dose by providing extra shielding of the source and by minimizing the production of both the scatter radiation and lead x-rays. If the flood source must be placed below the camera head (face down), the radiation dose to the technologist can be reduced by minimizing the distance between the source and the camera head. The nuclear medicine technologist also should employ other basic radiation safety precautions, such as working efficiently to reduce the time of exposure, increasing the distance between themselves and the source when possible, and using portable radiation shields.

REFERENCES

1. Steves AM. Instrumentation quality assurance. In: Steves AM, ed. *Review of Nuclear Medicine Technology*. 2nd ed. Reston, VA: Society of Nuclear Medicine; 1996:19–26.
2. Graham LS. Quality assurance procedures. In: Simmons GH, ed. *The Scintillation Camera*. Reston, VA: Society of Nuclear Medicine; 1988: 79–98.
3. NEMA. *Performance Measurements of Scintillation Cameras*. Publication No. NU1. Washington, DC: National Electrical Manufacturers Association; 1994.
4. Greaves CD, Tindale WB. Dose rate measurements from radiopharmaceuticals: implications for nuclear medicine staff and for children with radioactive parents. *Nucl Med Commun*. 1999;20:179–187.
5. McElroy NL. Worker dose analysis based on real time dosimetry. *Health Phys*. 1998;74:608–609.
6. Prussin SG, Theofanous G, Casey D, Kim A. Dose from syringe procedures during technetium-99m radiopharmaceutical preparation. *J Nucl Med Technol*. 1998;26:32–37.
7. Chiesa C, De Sanctis V, Crippa F, et al. Radiation dose to technicians per nuclear medicine procedure: comparison between technetium-99m, gallium-67, and iodine-131 radiotracers and fluorine-18 fluorodeoxyglucose. *Eur J Nucl Med*. 1997;24:1380–1389.
8. Hastings DL, Hillel PG, Jeans SP, Waller ML. An assessment of finger doses received by staff while preparing and injecting radiopharmaceuticals. *Nucl Med Commun*. 1997;18:785–790.
9. LaFontaine R, Graham LS, Behrendt D, Greenwell K. Personnel exposure from flood phantoms and point sources during quality control procedures. *J Nucl Med*. 1983;24:629–632.
10. Knoll GF. *Radiation Detection and Measurement*. 2nd ed. New York, NY: John Wiley; 1989.
11. Institute of Electrical and Electronics Engineers (IEEE). *Calibration and Use of Germanium Spectrometers for the Measurement of Gamma-Ray Emission Rates of Radionuclides*. ANSI N42.14–1991. New York, NY: IEEE; 1991.
12. Nix DW, Powers RP, Kanipe LG. *Application of Germanium Detectors to Environmental Monitoring*. US EPA report TVA/EP 79/06. Washington, DC: US Environmental Protection Agency, Office of Energy, Minerals and Industry; 1979.